catalysts

MDPI

Review

Recent Progress in the Production of Cyanide-Converting Nitrilases—Comparison with Nitrile-Hydrolyzing Enzymes

Ludmila Martínková [1,*], Natalia Kulik [1], Anastasia Sedova [2], Barbora Křístková [1,3] and Pavla Bojarová [1,2]

[1] Institute of Microbiology of the Czech Academy of Sciences, CZ-142 20 Prague, Czech Republic
[2] Department of Health Care and Population Protection, Faculty of Biomedical Engineering, Czech Technical University in Prague, CZ-272 01 Kladno, Czech Republic
[3] Faculty of Food and Biochemical Technology, University of Chemistry and Technology, Prague, Technická 5, CZ-166 28 Prague, Czech Republic
* Correspondence: martinko@biomed.cas.cz; Tel.: +420-296-442-569

Abstract: Nitrilases have a high potential for application in organic chemistry, environmental technology, and analytics. However, their industrial uses require that they are produced in highly active and robust forms at a reasonable cost. Some organic syntheses catalyzed by nitrilases have already reached a high level of technological readiness. This has been enabled by the large-scale production of recombinant catalysts. Despite some promising small-scale methods being proposed, the production of cyanide-converting nitrilases (cyanide hydratase and cyanide dihydratase) is lagging in this regard. This review focuses on the prospects of cyanide(di)hydratase-based catalysts. The current knowledge of these enzymes is summarized and discussed in terms of the origin and distribution of their sequences, gene expression, structure, assays, purification, immobilization, and uses. Progresses in the production of other nitrilase catalysts are also tackled, as it may inspire the development of the preparation processes of cyanide(di)hydratases.

Keywords: cyanide dihydratase; cyanide hydratase; cyanide removal; cyanide sensor; enzyme purification; immobilization; nitrilase; overexpression; phylogenetic analysis; whole-cell catalyst

Citation: Martínková, L.; Kulik, N.; Sedova, A.; Křístková, B.; Bojarová, P. Recent Progress in the Production of Cyanide-Converting Nitrilases—Comparison with Nitrile-Hydrolyzing Enzymes. *Catalysts* **2023**, *13*, 500. https://doi.org/10.3390/catal13030500

Academic Editor: Maria H. L. Ribeiro

Received: 20 December 2022
Revised: 3 February 2023
Accepted: 20 February 2023
Published: 28 February 2023

1. Introduction

Nitrilases (EC 3.5.5.-) represent a branch of the nitrilase superfamily [1]. They are also probably the only branch acting on cyanides or nitriles. The known members of the other branches are generally amidases.

The substrates of nitrilases are organic cyanides (nitriles) and/or HCN, which is a form of free cyanide (fCN). The HCN/CN^- ratio in fCN depends on pH. Two types of nitrilases prefer HCN as the substrate, the cyanide dihydratase (CynD) and cyanide hydratase (CynH). The latter is formerly classified as lyase (EC 4.2.1.66). Nevertheless, the classification of CynD and CynH as distinctive types of nitrilases is clearly justified by comparing their primary structures with those of nitrile-hydrolyzing enzymes (Table S1). In addition, the regions proximal to the key residues (Glu-Lys-Glu-Cys) are even more conserved, resulting in similar 3D structures (see below).

The two enzymes differ in their products, that is, formate and ammonia for CynD and formamide for CynH. Similarly, nitrilases transform nitriles into ammonia and carboxylic acid or amide or their mixture (Figure 1).

Some nitriles, typically 2-cyanopyridine (**1a**) and fumaronitrile (**2a**), are also transformed by CynHs (Figure 2).

While enzymatic hydrolysis of nitriles has been known since the 1950s, the first nitrilases that efficiently degrade HCN (CynHs) were reported about two decades later, followed by CynDs in the 1990s (see [1–3] for previous reviews).

The physiological role of nitrilases, including CynDs and CynHs, is not fully understood. It is generally supposed that the main functions of nitrilases are nitrogen recycling

and cyanide detoxification [4]. Specifically, one of the roles of CynHs in fungi is likely to be the detoxification of HCN released from cyanogenic glycosides that serve as plant defense compounds. It is plausible that the CynH product formamide can be hydrolyzed to provide ammonia. CynDs may serve similar purposes. The bacterial genera that produce CynDs are soil and plant-associated bacteria, which is consistent with this speculation.

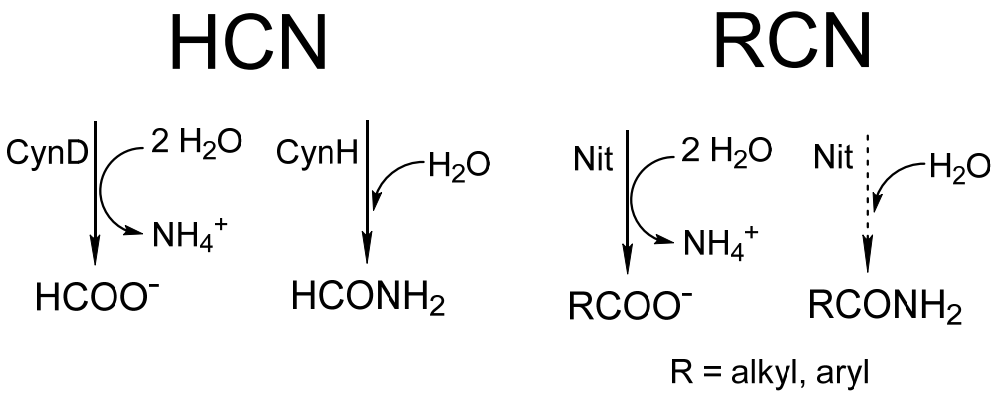

Figure 1. Conversion of hydrogen cyanide (HCN) by cyanide dihydratase (CynD) or cyanide hydratase (CynH), and conversion of nitriles (RCN) by nitrilase (Nit). CynHs also convert some nitriles at lower rates than those of HCN [2]. Unlike CynDs or CynHs, Nits include several subgroups with different substrate specificities [1].

Nitrilases can replace conventional tools of nitrile hydrolysis, such as strong acids or bases. They usually operate at pH 7–8 and 30–40 °C. They became attractive, especially because of their stereoselectivities and regioselectivities. A few nitrilase-catalyzed processes to produce fine chemicals were brought to a high degree of technological readiness (for relevant reviews, see [5–9]). For example, enantioselective hydrolysis of racemic mandelonitriles **3a** and **4a** provided (*R*)-mandelic acid (**3b**) [10] and its *o*-chloro derivative **4b** [11]. A regioselective hydrolysis of 1-cyanocyclohexaneacetonitrile (**5a**) provided 1-cyanocyclohexaneacetic acid (CCHA; **5b**) (Figure 2), the precursor of gabapentin (**3c**) [12], a widely used anticonvulsant medicine. In addition, many studies aimed at improving nitrilase catalysts by site-directed mutagenesis or immobilization (for relevant reviews, see e.g., [5,6,13,14]).

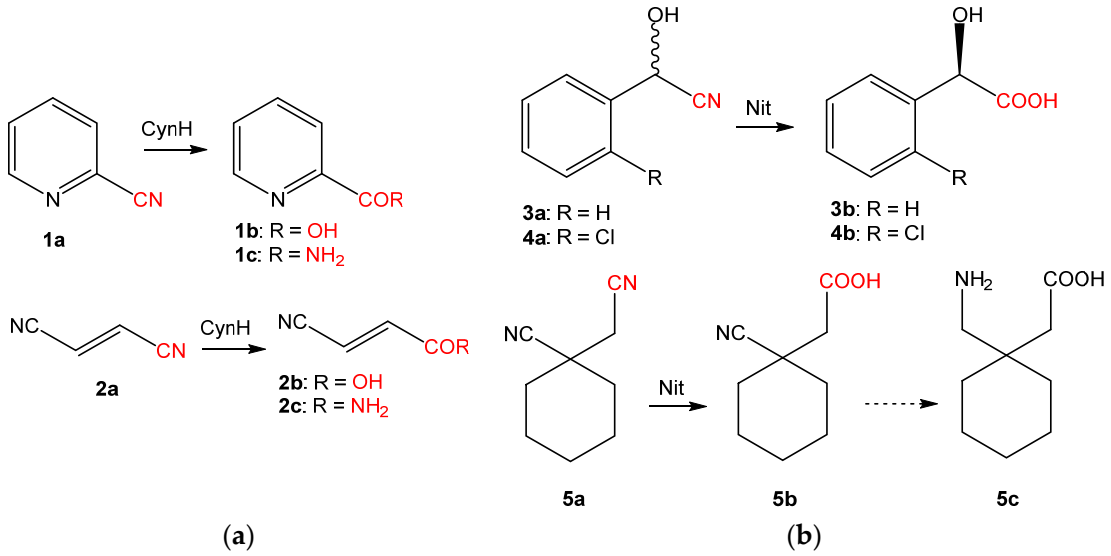

Figure 2. Examples of nitrile conversions by (**a**) cyanide hydratases (CynHs) and (**b**) nitrilases (Nits). CynHs produce carboxylic acids and/or amides from 2-cyanopyridine (**1a**) and fumaronitrile (**2a**).

The acid (**1b**,**2b**)/amide (**1c**,**2c**) ratio depends on enzyme origin [15]. Some bacterial Nits produce enantiopure *R*-mandelic acids **3b** and **4b** from (*R*,*S*)-mandelonitriles **3a** and **4a** [10,11], or 1-cyanocyclohexaneacetic acid **5b**, the precursor of gabapentin (**5c**), from the corresponding dinitrile **5a** [12].

In contrast, the production and application of CynHs or CynDs are less developed in terms of scale and catalyst improvement. Nevertheless, the potential of enzymes is promising for cyanide sensors and cyanide degradation in wastewaters from gold mining, metal plating, coking, chemical, and other industries. Previous comprehensive reviews on this topic summarized the literature up to about 2015 [2] and 2016 [3], with the latter focusing on the structure-activity relationships. Some general reviews on the removal of cyanide from wastewater also addressed the HCN-degrading enzymes [16,17]. Here, we summarize the main results obtained so far in this area, focusing mainly on the recent literature. We also address the major advances in the study of other nitrilases (nitrile-transforming enzymes) to the extent that they may provide new approaches for the development of HCN-degrading enzymes.

2. Origin and Distribution of the Sequences

CynDs are a relatively small group of enzymes. The two best-characterized ones are from *Bacillus pumilus* ($CynD_{pum}$) and *Pseudomonas stutzeri* ($CynD_{stut}$). These enzymes are about 80% identical (with a coverage of 95%) and differ mainly in their C-termini [18,19]. $CynD_{pum}$ and $CynD_{stut}$ seem strictly selective for HCN.

In addition, CynDs were recently reported in *Flavobacterium indicum* [20], *Bacillus safensis* [21], and *Bacillus* sp. [22]. The enzyme in *F. indicum* (here called $CynD_{ind}$) is different from the above-mentioned CynDs (its identity with $CynD_{pum}$ is only about 34% with a coverage of 92%). Moreover, it has a different sequence in the region containing the catalytically active cysteine residue, i.e., the ACGEN instead of the typical sequences of the well-known CynDs (MCWEH in $CynD_{pum}$ and $CynD_{stut}$). The number of non-redundant homologous sequences with 70–99% identity and ≥90% coverage to $CynD_{ind}$ is 151 in Flavobacteria (Table 1).

Table 1. Cyanide dihydratases (CynDs) identified in GenBank.

Phylum	Class	Genus	Sequences Found [1]	Species with Confirmed CynD Activity (Reference)
Firmicutes	Bacilli	*Bacillus*	52 [2]	*B. pumilus* [23–25]
		Paenibacillus	12 [3]	
		Other	4	
	Clostridia	*Clostridium*	6	
		Lacrimispora	1	
Proteobacteria	Gammaproteobacteria	*Acinetobacter*	1	
		Stutzerimonas	1	*S. stutzeri* [18]
	Betaproteobacteria	*Burkholderia*	2	
Actinobacteria	Actinomycetia	*Brevibacterium*	1	
Bacteroidota	Flavobacteria	*Flavobacterium*	147	*F. indicum* [20]
		Other	5	
Ascomycota	Saccharomycetes	*Scheffersomyces*	1	

[1] The templates were CynDs from *Bacillus pumilus* ($CynD_{pum}$, GenBank: AAN77004.1), *Stutzerimonas stutzeri* ($CynD_{stut}$, GenBank: BAA11653.1) and *Flavobacterium indicum* ($CynD_{ind}$, Genbank: CCG52320.1). Identity and coverage thresholds were 70–99% and 90%, respectively. [2] *Bacillus safensis*—17, *Bacillus pumilus*—15, *Bacillus thuringiensis*—5, and *Bacillus cereus*—4. [3] *Paenibacillus alvei*—8.

The GenBank database (https://blast.ncbi.nlm.nih.gov; accessed on 5 December 2022) contains 230 CynD sequences with ≥70% identity and ≥90% coverage to the templates

(Table 1), $CynD_{pum}$, $CynD_{stut}$ (*P. stutzeri* was reclassified as *Stutzerimonas stutzeri*), or $CynD_{ind}$ (233 including the templates). The number of non-redundant sequences with 70–99% identity to $CynD_{pum}$ or $CynD_{stut}$ is 79 (81 including the templates). We assume that CynD activity is likely in these proteins. However, it is difficult to speculate on those that have lower levels of identity (approximately 70 sequences more if the identity threshold is set at 50%). CynD sequences are frequently found in the genus *Bacillus* (52), and here mainly in the species *Bacillus pumilus* (15) and *Bacillus safensis* (17). All *Flavobacterium* homologs were joined in one clade with a significant phylogenic distance from other CynDs (see Figure S1 for the phylogenetic tree).

All putative CynDs found were of bacterial origin with one exception, which is the hypothetical CynD of the yeast *Sheffersomyces stipitis* CBS 6054. The closest homologs of this protein are bacterial proteins annotated as carbon-nitrogen hydrolase family proteins in *Clostridium ljungdahlii* (GenBank: WP_063554590.1) with ca. 76% identity and 96% coverage, and *Bacillus australimaris* (GenBank: MBR8688472.1) with ca. 74% identity and 97% coverage. The closest fungal homologs are hypothetical proteins from *Aureobasidium melanogenum* (GenBank: KAH0440800.1) with ca. 41% identity and 88% coverage and a putative nitrilase from *Hyaloraphidium curvatum* (GenBank: KAI9027987.1) with ca. 36% identity and 93% coverage.

The group of CynHs is larger (see Figure S2 for the phylogenetic tree) and more sequences were confirmed to have the expected activity. The recombinantly produced CynHs originated from *Fusarium lateritium* [26], *Aspergillus nidulans*, *Neurospora crassa*, *Gibberella zeae*, *Gloeocercospora sorghi* [27] (reclassified as *Microdochium sorghi*), *Aspergillus niger*, *Penicillium chrysogenum* [28], *Botryotinia fuckeliana*, *Pyrenophora teres* [29], *Stereum hirsutum* [15], and *Exidia glandulosa* [30]. Some other CynHs were directly obtained from their natural producers (for relevant reviews, see [2,31]). Homology searches were based on some annotated CynHs. The searches for sequences with 60–99% identity to selected confirmed CynHs and more than 90% coverage provided 389 homolog sequences (including the templates), with all of them in fungi and 98.5% of them in Ascomycota (Table 2). Only six of them were identified in Basidiomycota.

In contrast to CynDs, CynHs can also transform some organic cyanides. For example, the activities for 2-cyanopyridine (**1a**) and fumaronitrile (**2a**) (Figure 2) were found in all tested CynHs [28–30,32]. The V_{max}/K_M ratio is higher for HCN than for cyanopyridine or fumaronitrile in CynH from *A. niger* (ca. 62, 2.8, and 1.3, respectively) [32].

Table 2. Cyanide hydratases (CynHs) identified in GenBank.

Phylum	Class	Genus [1]	Sequences Found [2]	Species with Confirmed CynHs (Reference)
Ascomycota	Dothideomycetes	*Aureobasidium*	39	
		Alternaria	17	
		Hortaea	12	
		Pyrenophora	4	*P. teres* [29]
		Leptosphaeria	2	*L. maculans* [33]
		Stemphylium	1	*S. loti* [34]
		Other	46	
	Lecanoromycetes	*Mycoblastus*	2	
		Letharia	2	
		Other	6	
	Leotiomycetes	*Botrytis*	8	
		Monilinia	4	
		Botryotinia	1	*B. fuckeliana* [29]
		Other	20	

Table 2. *Cont.*

Phylum	Class	Genus [1]	Sequences Found [2]	Species with Confirmed CynHs (Reference)
	Sordariomycetes	*Fusarium*	43	*F. solani* [35], *F. lateritium* [26], *F. graminearum* [27] [3]
		Colletotrichum	21	
		Monosporascus	8	
		Diaporthe	6	
		Verticillium	6	
		Neurospora	2	*N. crassa* [27]
		Microdochium	2	*M. sorghi* [27] [4]
		Other	39	
	Eurotiomycetes	*Aspergillus*	52	*A. nidulans* [27], *A. niger* [32]
		Penicillium	29	*P. chrysogenum* [28]
		Other	9	
	Xylobotryomycetes	*Cirrosporium*	1	
	Sareomycetes	*Sarea*	1	
Basidiomycota	Agaricomycetes	*Auricularia*	3	
		Stereum	2	*S. hirsutum* [15]
		Exidia	1	*E. glandulosa* [30]

[1] The templates were CynHs from *Fusarium solani* (GenBank: CAC69666.1) [35] and *Gloeocercospora sorghi* (annotated as *Microdochium sorghi* in NCBI; GenBank: AAA33353.1) [27]. Identity and coverage thresholds were 60–99% and 90%, respectively. Non-redundant sequences were filtered with the tool (https://web.expasy.org/decrease_redundancy/; accessed on 5 December 2022). [2] Only the genera with the highest number of sequences or with confirmed CynHs are shown for each class. [3] Formerly *Gibberella zeae*. [4] Formerly *Gloeocercospora sorghi.*

Thus, CynDs and CynHs form relatively small fractions of nitrilases. The total number of nitrilase homologs is in the thousands according to GenBank (*not shown*). CynD and CynH both contain the Glu-Lys-Cys triad characteristic of the nitrilase superfamily (C164, E48, and K130 in $CynD_{pum}$). Substrate positioning was studied in two amidases from the genus *Pyrococcus*, one of which was previously designated as a nitrilase. In these enzymes, another conserved Glu, together with Lys and the first Glu, contributes to the correct position of the substrate toward the catalytic Cys [36]. It is thus essential for activity, which is also shown by mutation studies on an amidase from *Geobacillus pallidus* [37]. Nitrilases, without excluding CynDs and CynHs, also contain this conserved second Glu residue (Figure 3), which corresponds to E137 in $CynD_{pum}$. The sequence close to the second Glu is more conserved in CynH than in CynDs. However, we can identify a common pattern for both types of enzymes: XER/KL, where X is the hydrophobic aliphatic residue. In the selected nitrilases, only the ER motif is conserved.

CynHs or CynDs do not appear to be parts of metabolic pathways such as the "aldoxime-nitrile pathway", although some genera of fungi (*Fusarium*, *Aureobasidium*, etc.) contain both (putative) aldoxime dehydratases (Oxds) [38] and CynHs abundantly. However, a typical substrate of nitrilases involved in the above pathway is phenylacetonitrile (a natural compound), while the activities of CynHs are negligible for this substrate [29,32].

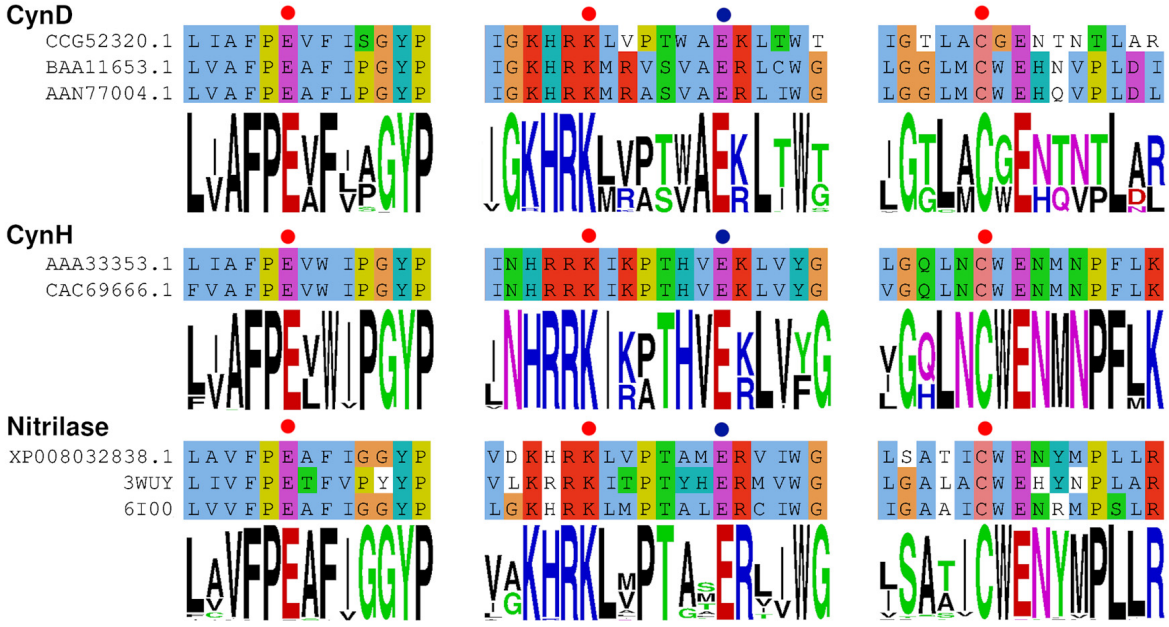

Figure 3. Sequence conservation diagrams of selected regions in cyanide dihydratases (CynDs) from *Flavobacterium indicum* (CCG52320.1), *Stutzerimonas stutzeri* (BAA11653.1) and *Bacillus pumilus* (AAN77004.1), cyanide hydratases (CynHs) from *Microdochium sorghi* (AAA33353.1) and *Fusarium solani* (CAC69666.1), and nitrilases (not utilizing HCN as substrate) from *Trametes versicolor* (XP_008032838.1), *Synechocystis* sp. (3wuy), and *Arabidopsis thaliana* (pdb 6i00). Red dots mark active site residues. Blue dots mark the second Glu of the catalytic tetrad. The alignment was constructed using CLUSTAL Omega. The diagrams were constructed with WebLogo (http://weblogo.berkeley.edu/logo.cgi). Active site amino acids were identified based on the previous study [1].

3. Overexpression of Genes

The *cynD* and *cynH* genes were obtained by the amplification of genomic, complementary [27,32,39], or synthesized DNA [28–30]. Their expression largely followed standard protocols with *Escherichia coli* as the host, although it differed in methodological details such as the cultivation medium, temperature regime, IPTG concentration, etc., as shown in Table 3 and Figure 4.

The two best-characterized CynDs ($CynD_{pum}$ and $CynD_{stut}$) were produced with an *N*-terminal His_6-tag, which slightly affected the kinetic parameters and the temperature optimum, as shown in $CynD_{pum}$ [39].

Some *cynH* genes were produced in the autoinduction medium (glucose, glycerol, and lactose [40]). Expression levels were similar for the tagged and untagged constructs. Subsequent work was carried out with the tagged constructs to simplify purification [27].

For enzyme overproduction in *E. coli*, recent studies on other nitrilases have proposed methods to increase efficiency and reduce cost. One promising approach is the high-density culture (the optical density was up to 86.4 at 600 nm). In addition, the *nit* gene (from *Pseudomonas putida*) was expressed constitutively, showing a high activity per liter of culture medium (654,000 U/L for 3-cyanopyridine as the substrate) [41].

The activity and stability of nitrilase can be improved by the chaperones GroEL/GroES. This was shown for a nitrilase from *Rhodococcus rhodochrous* produced in *E. coli* or *Rhodococcus ruber*. From the different options tested (fusion of each chaperone with nitrilase, co-expression), the co-expression of GroEL (in *R. ruber*) was the most effective; it increased the specific activity and, especially, the thermostability of the nitrilase (the latter by eightfold) [42]. The GroEL/GroES co-expression was also used for the production of CynHs and other nitrilases [29] (Table 3). Earlier investigation suggested the positive effect of these chaperones on nitrilase solubility [43,44].

Table 3. Overexpression of the *cynD* and *cynH* genes in *Escherichia coli*.

Enzyme	Vector; His_6-Tag	Medium; Cultivation Conditions	Kinetic Parameters	Reference
CynD	pET28a; *N*-terminal	LB broth; (i) 37 °C → OD 0.3; (ii) 1 mM IPTG, 30 °C, 3–4 h	V_{max} 120–150 U/mg [2] K_M 0.7–7.9 mM [2]	[18,19,45]
CynH	pET26b; *C*-terminal	LB broth; (i) 30 or 37 °C → OD 0.5; (ii) 1 mM IPTG, 30 °C, 3–10 h	V_{max} ≈ 4400 U/mg [3] K_M ≈ 90 mM [3]	[39]
	pET28a; *N*-terminal pET26b; no tag	Autoinduction medium (g/L): glucose 0.5, glycerol 5, lactose 2; 30 °C, overnight	n.d.	[27]
	pET30a; no tag	LB broth; (i) 37 °C → OD 0.4–0.6; (ii) 0.8 mM IPTG, 26 °C, 16 h	V_{max} ≈ 6800 U/mg [4] K_M ≈ 109 mM [4]	[32]
	pET22b, pGro7 (Takara) [1]; *C*-terminal	EnPresso (Biosilta); (i) 30 °C, 16 h; (ii) 0.02 mM IPTG, 11 mM L-arabinose; 25 °C, 24 h	n.d.	[29]
	pET22b; *C*-terminal	2xYT; (i) 37 °C → OD 1.0; (ii) 0.02 mM IPTG, 20 °C, 20 h	V_{max} ≈ 1335 U/mg [5] K_M ≈ 22 mM [5]	[30]

[1] Encoding GroEL/ES chaperone (expression induced by L-arabinose). [2] *Bacillus pumilus* CynD and mutants. [3] *Gloeocercospora sorghi* (reclassified: *Microdochium sorghi*). [4] *Aspergillus niger*. [5] *Exidia glandulosa*. n.d., no data.

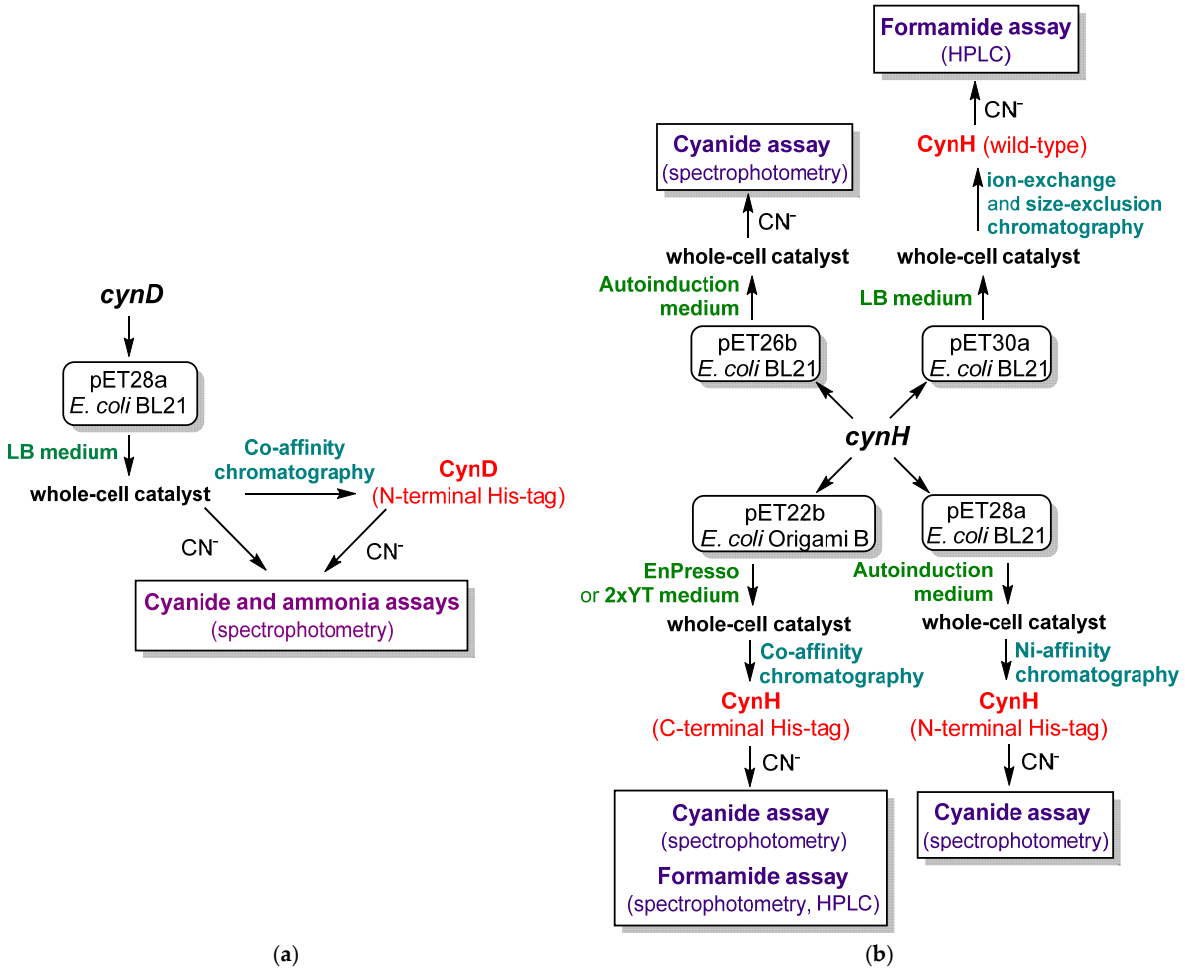

Figure 4. Summary of the methods used for the production, purification, and activity assays used for (**a**) cyanide hydratases (CynDs) and (**b**) cyanide hydratases (CynHs). See Tables 3 and 4 for the details of gene expression and activity assays, respectively.

Table 4. Cyanide (di)hydratase activity assays.

Enzyme/Reaction Conditions	Compound Determined	Reagent	Method	Reference
CynD/4 mM KCN, pH 7.7, r.t.	Free cyanide	Picric acid, Na_2CO_3	Spectrophotometric	[18,19,45]
CynD/4 mM KCN, pH 7.7, r.t.	Ammonia	Nessler (K_2HgI_4)	Spectrophotometric	[18]
CynH/10 mM KCN, pH 7.4, r.t.	Free cyanide	Picric acid, Na_2CO_3	Spectrophotometric	[27]
CynH/25 mM KCN, pH 8.0, 30 °C	Formamide	-	HPLC (ion-exchange column)	[32]
CynH/25 mM KCN, pH 8.0, 30 °C	Formamide	-	HPLC (silica gel column)	[15]
CynH/25 mM KCN, pH 9.0, 30 °C	Formamide	(i) Hydroxylamine/NaOH, (ii) HCl/$FeCl_3$	Spectrophotometric	[30]

r.t., room temperature.

The above cultivations were carried out on small scale. However, the feasibility of scaling up the production of a related enzyme (nitrilase acting on mandelonitrile) was demonstrated for *E. coli* harboring the *nit* gene from *A. faecalis* [10]. The whole-cell catalyst produced *R*-MA from 0.5 M *(R,S)*-mandelonitrile. The cells were prepared in 420 L, 4200 L, and 12,000 L of an autoinduction medium.

There are only very few examples of the use of *Pichia pastoris* (reclassified as *Komagataella phaffii*) as the host for *nit* gene expression. However, this host organism has some significant advantages in post-translational modification, and restricted leakage and solubility of the recombinantly produced protein [46]. The associated approach has been demonstrated with nitrile-hydrolyzing enzymes [46–48].

The nitrilase production in *K. phaffii* was intracellular [46,47] or extracellular [48]. Thus, this host was used to co-express the *nit* gene of *Pseudomonas fluorescens* and the oxynitrilase gene from *Manihot esculenta*, and the whole-cell catalyst was used for the biocatalytic synthesis of (*S*)-mandelic acid from benzaldehyde [47]. An efficient and robust nitrilase for the production of CCHA was also prepared in *K. phaffii*. The strain carried multiple copies of the *nit* gene from *Acidovorax facilis*. In addition, the production was optimized by selecting a suitable (alcohol oxidase 1) promoter and co-expressing a chaperone (ER oxidoreductin 1). The resulting whole-cell catalyst was quite stable for one day at 55 °C and could be used for at least 20 times [46]. Another strain of this organism produced the nitrilase from *Alcaligenes faecalis* for the synthesis of *R*-MA from mandelonitrile; the enzyme was produced constitutively and secreted into the culture medium [48].

4. Activity Assays

The assays of cyanide-transforming enzymes are based on different principles (Table 4 and Figure 4), and the use of different methods can make it difficult to compare the results. The activities of CynDs or CynHs were often determined based on the rate of substrate (fCN) consumption. However, the fCN concentrations or pH were different in different studies. Alternatively, the rate of product (ammonia and formamide) formation was used. In CynHs, the concentration of substrate was often lower than K_M. The K_M values of CynHs are very high (up to ~100 mM, Table 3) [2]. Therefore, the specific activities may be underestimated. In addition, the temperature and pH can affect the stability of fCN, which evaporates significantly at a pH of 8.5 or lower [49].

For example, CynDs were tested with 4 mM fCN at pH = 7.7, and the consumption of fCN was determined with the picric acid reagent [18,19,45]. Alternatively, the product ammonia was determined using the Nessler reagent under the same conditions [18] or at a pH ranging from 5.5 to 9.5 [19].

The activities of the first recombinant CynHs were determined using 10 mM KCN at pH = 4.5–11. In stability assays, the residual activities of the enzymes were determined at pH = 7.4. The concentrations of the remaining fCN were monitored using the picric acid reagent [27]. The activity of a new CynH from *E. glandulosa* was determined with 25 mM KCN at pH = 9–10.5, and the residual fCN was determined in the same way. The formation of formamide was monitored spectrophotometrically using the hydroxylamine reagent according to a previous method [50]. At pH = 9.0, the 22 mM formamide was obtained from 25 mM KCN after 1 h. The rest of the substrate was probably lost by evaporation. However, the activities calculated from the consumption of fCN and the formation of formamide were comparable after 1 to 2 min of reactions at pH = 9.0 and 30 °C [30]. Alternatively, the concentrations of the formed formamide were determined by HPLC/UV using an ion exchange column [28]. The formamide can also be analyzed by HPLC/UV using a silica gel column [51] and this method was used with the CynH from *S. hirsutum* [15]. However, the sensitivity of the methods is low due to the low UV absorbance of formamide.

5. Structural and Computational Studies

The first CynD structure was resolved for a $CynD_{pum}$ mutant (Q86R, H305K, H308K, H323K) recently (pdb code 8c5i, deposition date 18 January 2023). Most previous studies were based on homology models and were optionally combined with electron microscopy. These approaches were used for mutation analyses and predictions of molecular contact surfaces (interfaces) or C-termini (see below).

In their active form, nitrilases are largely oligomers of 4 to 22 subunits. In addition, some produce extended spirals of different lengths [1]. The active form of $CynD_{pum}$ is a helical oligomer comprised of 18 monomer units [52]. The number of subunits in the similar structure of $CynD_{stut}$ is 14 [53]. Active nitrilase monomers have been rarely reported. One of them is the recently described CynD from *Flavobacterium indicum* [20].

The contact interfaces between the monomers in a helical oligomer are designated A, C, D, and E, whereas in nitrilase Nit4 from *Arabidopsis thaliana*, the F interface has also been found, which depends on oligomer termination [54]. The positions of A, C, and D surfaces for Cyn_{pum} are shown in Figure 5a (the E interface is formed by the rotation of the terminal dimers in the helix).

The C interface contains residues 55–72 and 222–235 in $CynD_{pum}$ (54–71 and 221–234 in $CynD_{stut}$) [24]. The length of the first C-interface loop is similar for all the identified homologs, with the conserved motif YP[W/Y] at the beginning of the loop. The importance of these regions for oligomerization and activity has been demonstrated by mutation studies [23,24,55] (Section 6).

The C-termini, which are part of the A interface, also maintain interactions required for the formation of the quaternary structure in nitrilases. They span at least two adjacent dimers in Nit4 from *Arabidopsis thaliana* (pdb 6i00) [54] and the nitrilase from *Pseudomonas fluorescens* EBC191 (pdb 6zby). The orientation of the C-terminus in the dimer of the recently reported structure of $CynD_{pum}$ is shown in Figure 5b. This C-terminus is longer than that in Nit4 (see the multiple alignment in Figure 5c) and spans three adjacent dimers (Figure 5b).

A conserved motif D[P/F]XGHY [1] was identified for C-termini in bacterial, fungal, and plant nitrilases (Figure 5c). In contrast to $CynD_{stut}$, $CynD_{pum}$ and their homologs (in which this motif is conserved) the CynD of *F. indicum* and its homologs (with only one outlier sequence) have a DILGHY motif and a shorter C-terminus (Figure 5c).

CynHs are also multimers [1]. The structure of CynH has not yet been elucidated, and thus, most studies rely on homology models reported for, e.g., the CynHs from *N. crassa* [1] and *Stereum hirsutum* [15]. The lengths of the sequences that form the C interface are similar for CynHs and CynDs. A conserved motif YP[W/Y] is present in most of the identified CynH homologs, except for three sequences. The presence of a WPV motif in the active site of CynH limits the size of substrates that can be accepted by CynHs [15].

The corresponding sequence in $CynD_{pum}$ is $W^{188}PG^{190}$. The C-terminus in CynH homologs has a conserved motif (DXXGHY) similar to that of CynDs (Figure 5c).

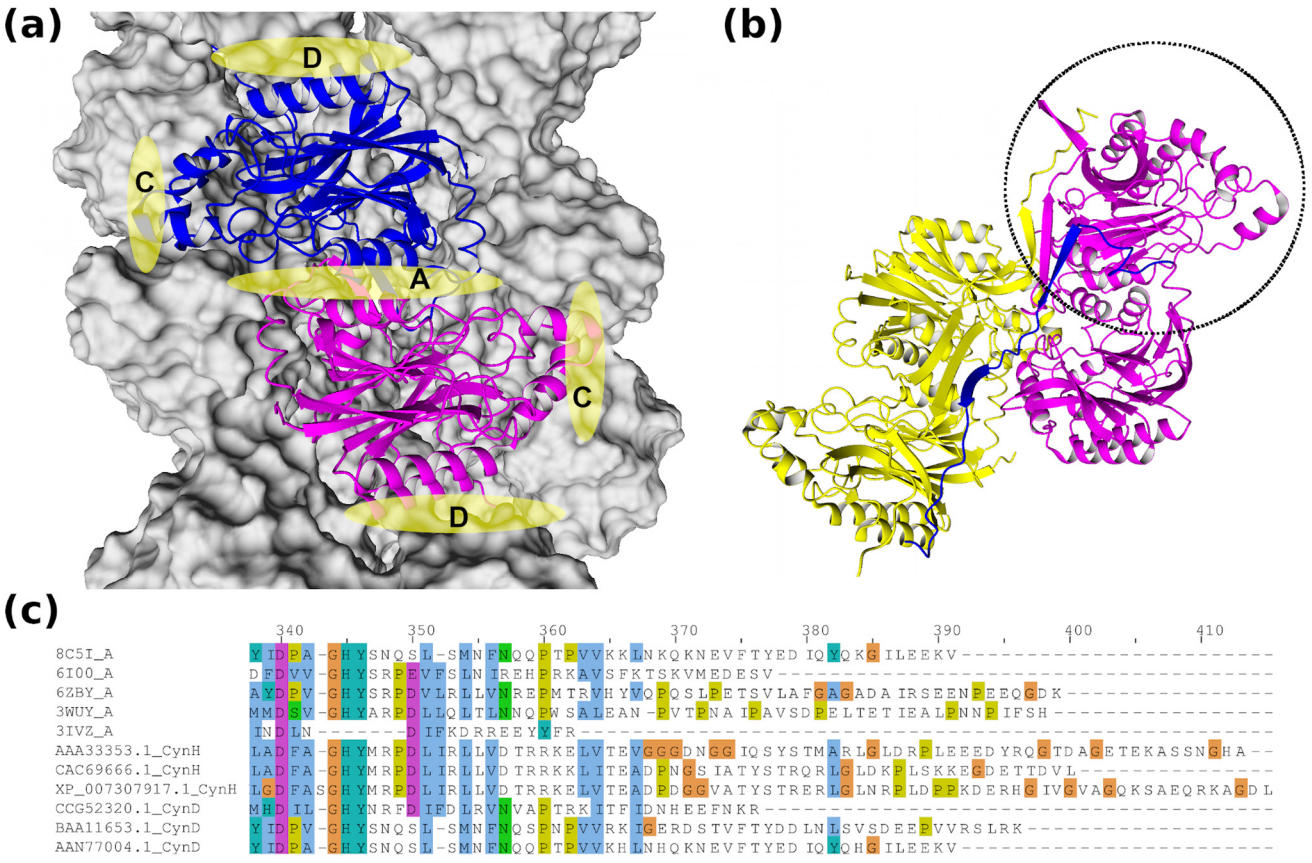

Figure 5. (**a**) Contact interfaces in the helical form of $CynD_{pum}$. The monomers in one of the dimers are shown in magenta and blue and the rest of the helix is shown by surface representation. Contact interfaces are highlighted in yellow and labeled. The A interface is formed between monomers in a dimer, the C interface is formed between two dimers in the helix, and the D interface is formed between helical turns. (**b**) Adjacent dimers (colored differently). The C-terminal part of the encircled monomer is highlighted in blue to visualize its 3-D orientation. (**c**) Multiple sequence alignment of the C-terminal regions of $CynD_{pum}$ mutant (pdb 8c5i), Nit4 from *Arabidopsis thaliana* (pdb 6i00) [54], nitrilase from *Pseudomonas fluorescens* EBC191 (pdb 6zby), nitrilase from *Synechocystis* sp. PCC6803 (pdb 3wuy) [56], nitrilase-superfamily enzyme from *Pyrococcus abyssi* (pdb 3ivz) reclassified from nitrilase to amidase [36], CynH from *Microdochium sorghi* (AAA33353.1) [27], CynH from *Fusarium solani* (CAC69666.1) [35], CynH from *Stereum hirsutum* (XP_007307917.1) [15], CynD from *Flavobacterium indicum* (CCG52320.1) [20], CynD from *Stutzerimonas stutzeri* (BAA11653.1), and CynD from *Bacillus pumilus* (AAN77004.1) [24,55].

6. Engineered Enzymes

The potential of enzyme improvement by mutations was described for CynDs. Although the methodology was based on random mutagenesis in some cases, it was largely based on site-directed mutagenesis of the contact interfaces (mainly A and C) and the C-terminus. These mutations mainly altered the pH range, thermostability, and oligomerization/activity of the enzymes (see Section 6.1., Section 6.2. and Section 6.3., respectively). However, similar studies are still largely lacking for CynHs. In contrast, mutations in the contact interfaces or C-termini were also reported for nitrilases [54,57].

Several nitrilase mutations may also be relevant to CynDs or CynHs. For example, the mutants that alter the reaction product toward amide were studied in detail for the nitrilase from *Pseudomonas fluorescens* [13]. A similar change in the product was achieved in the

nitrilase from *Synechocystis* sp. by replacing F193 with Asn [58]. In contrast, mutations of several residues in the active site environment (e.g., mutation of the second key glutamate E142 to Ala) in this enzyme resulted in a loss of catalytic activity tested toward fumaronitrile, 2-butenenitrile, benzonitrile, 2-cyanopyridine, and 3-cyanopyridine [56].

6.1. Improvement of the pH Range

A hybrid (called $CynD_{pum\text{-}stut}$) was created with the C-terminal part of $CynD_{pum}$ being replaced by that of $CynD_{stut}$ [19]. It exhibited a different pH profile compared to the wild-type CynDs. The mutant was highly active at pH = 9.0 and fairly active at pH = 9.5. Moreover, unlike the wild-type enzymes, it retained some activity at pH = 10.0. Other mutants with improved activity at alkaline pH were produced by point mutations [59], although they were outperformed by the above hybrid (Table 5).

Table 5. Improved variants of cyanide dihydratase from *Bacillus pumilus* ($CynD_{pum}$).

Variant	Increased Thermostability	Activity at pH $\geq$ 9.0	Reference
K39R	+	(+)	[45]
Q86R	++	+	[59]
D172N	(+)	-	[45]
E327K	(+)	(+)	[45]
E327G	-	++	[59]
E35/Q322R/E327G	-	++	[59]
Q86R/E96G/D254E	+	++	[59]
Q86R/E96G/D254E/E327G	+	++	[59]
K39R/D172N/E327K	++	-	[45]
307NHQKNE312 replaced with GERDST [1]	+	(+)	[19]
$CynD_{pum\text{-}stut}$ hybrid [2]	++	++	[19]
$CynD_{pum\text{-}stut}$ K39R	+++	++	[19]

[1] Corresponding sequence (306–311) in $CynD_{stut.}$ [2] The $CynD_{pum\text{-}stut}$ contained 286 residues of $CynD_{pum}$ and the C-terminus of $CynD_{stut}$ (from residue 287 to end).

In contrast, some wild-type CynHs are quite active at pH = 9.0 or higher [27,30]. Therefore, their improvement is not so urgent in terms of pH ranges.

6.2. Stability Enhancement

The stability of wild-type CynDs and their mutants was examined at 42 °C. In general, the purified protein (10 μg/mL) was incubated at pH = 7.7 for 1 or 2 days. The hybrid $CynD_{pum\text{-}stut}$ retained 50% of the initial activity after 17 h at 42 °C, whereas the wild-type CynDs retained 50% of activity after 1 h [19].

The GERDST motif in the C-terminus of $CynD_{pum}$ had a positive effect on the thermostability of $CynD_{pum}$ [19]. The significance of the individual amino acid residues in the GERDST motif in $CynD_{pum}$ (not conserved, Figure 5c) was investigated using alanine scanning. All mutants retained activity, but three of them were much less active than the wild-type $CynD_{stut}$ [18].

The thermostability of the hybrid was further improved by a point mutation when K39 was replaced by R [19]. The K39R mutant of $CynD_{pum}$ was selected among those produced by the error-prone PCR. Two other mutants (E327K and D172N) also showed improved thermostability, whereas the K39R/D172N/E327K triple mutant was still better [45].

Some wild-type CynHs are quite thermostable. The CynH from *N. crassa* showed the highest thermostability of the four CynHs tested, with 40% of residual activity after 2-day incubation at 43 °C [27].

6.3. Mutants with Altered Oligomerization and Activity

Mutations in the regions that form the A- and C-surfaces (Section 5) have been studied, and some of them have been shown to affect activities. Complete deletion of residues

220–234 (the C surface) in $CynD_{stut}$ (219–233 in $CynD_{pum}$) resulted in inactive forms. Mutation of residues 55–72 (another part of the C surface) in $CynD_{pum}$ resulted in up to >90% activity loss. Some of these mutants, such as R67C, formed smaller oligomers including a dimer [24]. In contrast, the Y70C mutant showed a normal oligomer size (18 subunits) despite no activity. This suggested another mechanism of action that disabled CynD from reaching the desired conformation [23].

The $CynD_{pum}$ mutants with shortened C-terminal parts (the A surface) exhibited decreased activities. Mutants terminated at residues 303 and 293 retained 87% and 27% activity of the wild-type enzyme (330 residues), respectively. The mutant with only 279 residues was inactive. Similar studies were performed for deletion mutants of $CynD_{stut}$ (334 residues) in which residues after 330, 310, and 302 were removed. The mutants had residual activities of 97%, 13%, and 0%, respectively [18].

Similar trends were observed for CynH from *N. crassa* (351 residues; deletion of residues after 339, 323, and 307). The mutants showed residual activities of 46%, 22%, and 0%, respectively [18]. Mutants of CynH of *A. niger* (356 residues) showed similar behaviors. Deletion of 14 residues of the C-terminus had no significant effect on activity, but deletion of 18 or more residues (after residue 338, 334, or 322) had nearly abrogated activity [32]. The exact position of the C-terminus in $CynD_{pum}$ has been determined for the recently resolved structure (8c5i). The role of the C-terminal part is likely to be similar to that reported for the Nit4 nitrilase (pdb 6i00) (see Section 5).

The effect of the A and C surfaces on the nitrilase conformation was also discussed in a previous study on plant nitrilases. Two plant nitrilases were manipulated by combining ("swapping") their fragments with additional modifications of the above surfaces. This not only improved the catalytic properties but also increased the solubility of the resulting mutant [60]. Thus, these findings could have broader applications in nitrilases.

7. Catalyst Forms and Uses

The recombinantly produced CynDs and CynHs were largely purified by affinity chromatography [18,19,27,29,30,45] (Figure 4). The purification yields were rarely reported. The yield was reported to be 14.4% for the CynH from *E. glandulosa* using cobalt affinity chromatography [30]. In contrast, the CynH from *A. niger* did not contain a tag and was purified in two steps (ion exchange chromatography and size exclusion chromatography). The purification yield was 17% [32].

The purified $CynD_{pum}$ was maintained at −80 °C [19]. In contrast, these conditions were not suitable for the purified CynHs due to the precipitation of the enzyme [27]. Therefore, the CynHs were stored at 4 °C [27,30]. Thus, the CynH from *E. glandulosa* retained over 4/5 of its activity after more than three months under these conditions [30].

The purified CynHs were tested for the detoxification of fCN in samples of real industrial wastewater or model samples (Table 6). For example, some of them were shown to be resistant to typical pollutants occurring together with free cyanide in coking or petrochemical wastewater (sulfide, thiocyanate, ammonia, and phenol) [30] or real coking wastewater [61] (Figure 6). Some were also active in the solutions of Ag or Cu salts mimicking diluted electroplating wastewaters [30] or diluted real wastewaters of this type [27] (Figure 7).

Studies on the immobilization of CynDs or CynDs are very few (Table 6). The whole cells of *E. coli* producing $CynD_{pum}$ were entrapped in agar or polyacrylamide and tested on a real mining effluent diluted to 17.6 mM fCN (Figure 8). Both catalysts almost completely degraded 5 mM fCN after 2 h. Moreover, the agar-immobilized catalyst could be reused many times (with 91% and 60% fCN conversion at cycles 22 and 30, respectively). In contrast, the cells immobilized with polyacrylamide showed lower operational stability (the conversion decreased rapidly after about five runs). Both were much more active than the free whole cells at pH = 9.0 and also retained almost full activity at pH = 10.0, where the free whole cells were virtually inactive [62]. This suggests that adopting immobilization

to protect the enzyme from the bulk medium is a useful alternative to the much more laborious mutations.

Table 6. Forms of catalysts for the degradation of free cyanide and their uses.

Enzyme	Catalyst Form	Properties	Application	Cyanide Concentration; Removal	Reference
CynD	Whole cells immobilized in agar	Recyclability (>20-fold); Activity at pH 9–10	Elimination of cyanide from mining waste	17.6 mM, 98% [1]	[62]
	Whole cells immobilized in polyacrylamide	Recyclability (5-fold); Activity at pH 9–10		17.6 mM, 98% [1]; 528 mM, 43% [2]	
CynD	Whole cells immobilized in agar	Optimal activity at pH 8.0, 35 °C Half-life 4 h at 40 °C	Cyanide sensor	n.a.	[63]
CynH	Whole cells in a flow reactor	Operational stability (3 days)	Elimination of cyanide [1]	25 mM, >80% [3]	[32]
CynH	Purified	Activity at up to pH 10; Prolonged shelf-life (>3 months)	Elimination of cyanide	0.6–100 mM; 96–100% [3]	[30]
	Purified	Activity at up to pH 10	Elimination of cyanide from electroplating waste	100 mM, 30–100% [4]	[27]

[1] Diluted wastewater. [2] Undiluted wastewater. [3] Model solution. [4] Lower conversion in the presence of copper than silver.

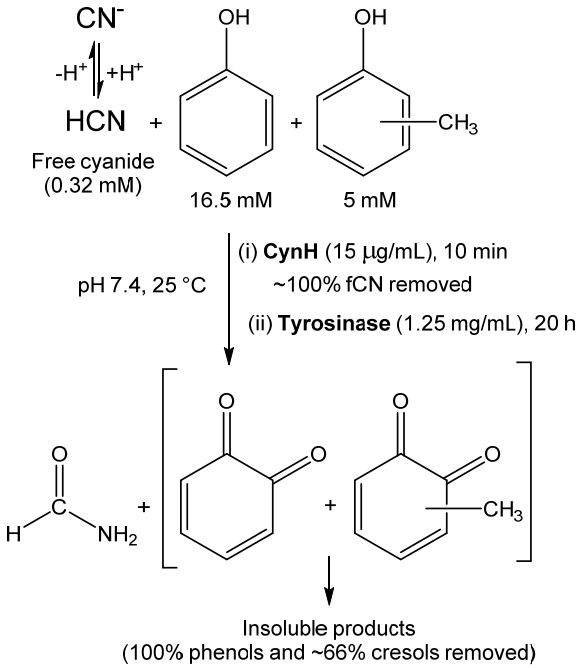

Figure 6. Removal of free cyanide (fCN) and phenol compounds (phenol, *m*-cresol, and *p*-cresol) from coking wastewater by cyanide hydratase (CynH) and tyrosinase, respectively. The reactions cannot proceed simultaneously due to the inhibition of tyrosinase (a copper enzyme) by fCN. Therefore, in the first step, fCN was converted to formamide by CynH overproduced in *Escherichia coli* and purified. In the second step, phenol compounds were degraded by the tyrosinase extracted from the fruiting bodies of *Agaricus bisporus*. Formamide, unlike fCN, was not inhibitory to tyrosinase [61].

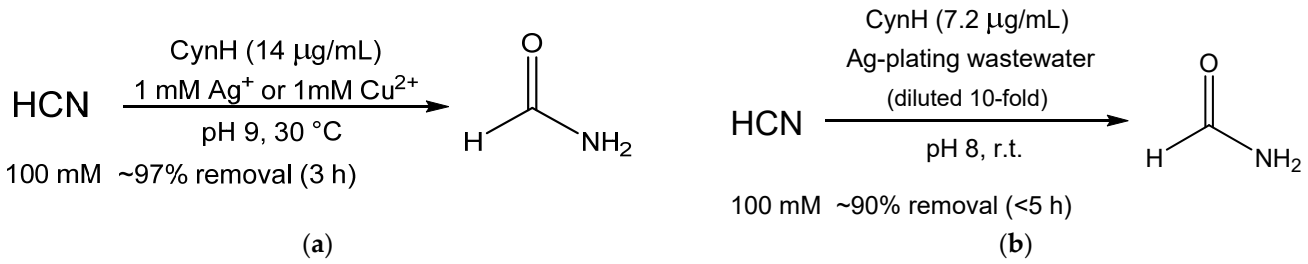

(**a**) (**b**)

Figure 7. Removal of free cyanide (depicted as HCN) in model or diluted real electroplating wastewaters by cyanide hydratases (CynHs) overproduced in *Escherichia coli*. (**a**) The model wastewater was 100 mM glycine/NaOH buffer at pH = 9.0, supplemented with 100 mM KCN and 1 mM of $AgNO_3$ or 1 mM $CuSO_4$. Conversion of HCN was catalyzed by the purified CynH from *Exidia glandulosa* [30]. (**b**) An electroplating bath wastewater with ca. 1 M fCN was 10 times diluted with 1 M MOPS buffer at pH = 8.0. Conversion of HCN was catalyzed by the purified CynH from *Neurospora crassa* [27]. The Cu or Ag content was not specified. r.t., room temperature.

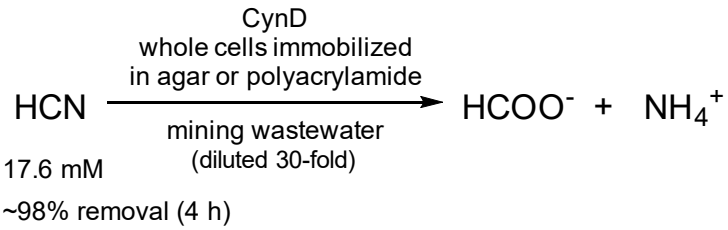

Figure 8. Biodegradation of free cyanide (depicted as HCN) in diluted gold-mining wastewater ("barren solution", i.e., the solution from which no more gold can be obtained) by immobilized whole-cell catalyst based on the cyanide dihydratase (CynD) from *Bacillus pumilus*. The enzyme was overproduced in *Escherichia coli* and used as whole cells immobilized in agar or polyacrylamide beads [62].

Immobilized CynDs were also proposed to be used in cyanide biosensors as summarized previously [2]. In addition, a new biosensor was proposed based on the CynD from *F. indicum* [63] (Figure 9).

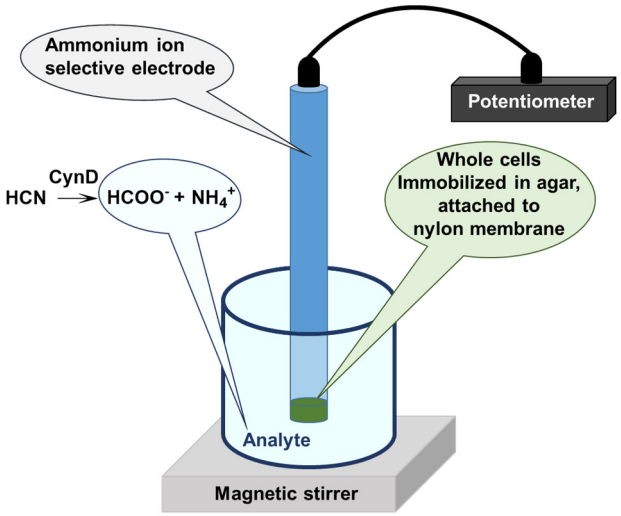

Figure 9. Potentiometric determination of free cyanide (fCN, depicted as HCN) using whole cells of *Flavobacterium indicum* with cyanide dihydratase (CynD) activity. The cells were entrapped in agar and the resulting catalyst was adsorbed on a nylon membrane. The sensor was used to determine fCN concentrations between 1.5×10^{-9} and 2.5×10^{-3} M [63].

The CynH from *A. niger* was used in the form of a whole-cell catalyst held in place by a semipermeable cellulose membrane. The reaction was carried out in a bench-scale flow reactor fed with a solution of 25 mM KCN. The conversion was maintained above 80% for 3 days [32].

The CynHs also act on organic cyanides, and therefore, their uses for synthetic purposes may be possible. For example, a few CynHs exhibited significant activities for 2-CP, which is not well accepted by most of other nitrilases [28]. The major product of this reaction is picolinic acid (fine chemical for synthesis, L-Trp metabolite, biomarker in neurological, and other diseases [64]).

Recent studies on the different types of nitrilases have shown other immobilization methods, such as encapsulation of purified nitrilase in biosilica [65], a modification of an earlier method [66], or cross-linked enzyme aggregates [67], a type of immobilized catalyst first proposed by the Sheldon group [68,69].

8. Conclusions

In general, CynDs and CynHs represent small fractions of the large group of nitrilases. Both of them exhibit a significant sequence conservation except for their C-terminal parts. However, there is a fine line between CynDs and the nitrilases with other substrate specificities. A clear classification of the enzymes would help search for additional CynD candidates. CynDs and CynHs have several potential applications in environmental technology and analytics. The wild-type enzymes are highly active for fCN, although CynDs are relatively unstable. The enzymes can be substantially improved by creating artificial variants and by immobilization. Both approaches have been found successful with CynDs. Similar progress has not been achieved with CynHs. However, some CynHs with promising properties (activity at pH = 9–10, thermostability, and shelf-life) have been obtained directly by retrieving appropriate sequences from databases. Further engineering of the CynDs could be based on the recently deposited structure of a CynD. The next issue to be addressed is to achieve low-cost expression of the genes (e.g., by autoinduction as demonstrated for some CynHs) and its scale-up. The CynHs may also have applications in organic synthesis. The improvement and overexpression of CynDs and CynHs and the scale-up of their production could be inspired by the achievements reported for other nitrilases.

Supplementary Materials: The following supporting information can be downloaded at: https://www.mdpi.com/article/10.3390/catal13030500/s1, Table S1. Percentage of amino acid sequence identities between cyanide dihydratases, cyanide hydratases, and nitrile-converting nitrilases; Figure S1. Complete phylogenetic tree of cyanide dihydratase homologs; Figure S2. Complete phylogenetic tree of cyanide hydratase homologs [15,70–74].

Author Contributions: Conceptualization, L.M., N.K. and P.B.; methodology, N.K.; data curation, N.K.; writing—original draft preparation, L.M., N.K. and A.S.; writing—review and editing, L.M., N.K., B.K. and P.B.; supervision, L.M. and P.B.; project administration, L.M. and P.B.; funding acquisition, L.M., P.B. and A.S. All authors have read and agreed to the published version of the manuscript.

Funding: This research was funded by Czech Science Foundation, grant number GA22-06785S, Czech Technical University in Prague—Faculty of Biomedical Engineering, grant number SGS21/181/OHK4/3T/17, and Czech Academy of Sciences, grant number RVO61388971.

Data Availability Statement: The complete phylogenetic trees of cyanide dihydratases and cyanide hydratases are available at https://itol.embl.de/tree/14723125414320859167100562 1 (accessed on 20 December 2022) and https://itol.embl.de/tree/17825516828117701671187763 (accessed on 20 December 2022) respectively.

Conflicts of Interest: The authors declare no conflict of interest.

References

1. Thuku, R.N.; Brady, D.; Benedik, M.J.; Sewell, B.T. Microbial nitrilases: Versatile, spiral forming, industrial enzymes. *J. Appl. Microbiol.* **2009**, *106*, 703–727. [CrossRef] [PubMed]
2. Martínková, L.; Veselá, A.B.; Rinágelová, A.; Chmátal, M. Cyanide hydratases and cyanide dihydratases: Emerging tools in the biodegradation and biodetection of cyanide. *Appl. Microbiol. Biotechnol.* **2015**, *99*, 8875–8882. [CrossRef] [PubMed]
3. Park, J.M.; Sewell, B.T.; Benedik, M.J. Cyanide bioremediation: The potential of engineered nitrilases. *Appl. Microbiol. Biotechnol.* **2017**, *101*, 3029–3042. [CrossRef] [PubMed]
4. Howden, A.J.; Preston, G.M. Nitrilase enzymes and their role in plant-microbe interactions. *Microb. Biotechnol.* **2009**, *2*, 441–451. [CrossRef]
5. Martínková, L.; Rucká, L.; Nešvera, J.; Pátek, M. Recent advances and challenges in the heterologous production of microbial nitrilases for biocatalytic applications. *World J. Microbiol. Biotechnol.* **2017**, *33*, 8. [CrossRef]
6. Martínková, L.; Křen, V. Biocatalytic production of mandelic acid and analogues: A review and comparison with chemical processes. *Appl. Microbiol. Biotechnol.* **2018**, *102*, 3893–3900. [CrossRef]
7. Singh, R.V.; Sambyal, K. Green synthesis aspects of (*R*)-(-)-mandelic acid; a potent pharmaceutically active agent and its future prospects. *Crit. Rev. Biotechnol.* 2022, *online ahead of print*. [CrossRef]
8. Shen, J.D.; Cai, X.; Liu, Z.Q.; Zheng, Y.G. Nitrilase: A promising biocatalyst in industrial applications for green chemistry. *Crit. Rev. Biotechnol.* **2021**, *41*, 72–93. [CrossRef]
9. Chen, Z.; Zhao, J.; Jiang, S.Q.; Wei, D.Z. Recent research advancements on regioselective nitrilase: Fundamental and applicative aspects. *Appl. Microbiol. Biotechnol.* **2019**, *103*, 6393–6405. [CrossRef]
10. Zhang, X.H.; Wang, C.Y.; Cai, X.; Xue, Y.P.; Liu, Z.Q.; Zheng, Y.G. Upscale production of (*R*)-mandelic acid with a stereospecific nitrilase in an aqueous system. *Bioprocess Biosyst. Eng.* **2020**, *43*, 1299–1307. [CrossRef]
11. Wang, H.; Gao, W.; Sun, H.; Chen, L.; Zhang, L.; Wang, X.; Wei, D. Protein engineering of a nitrilase from *Burkholderia cenocepacia* J2315 for efficient and enantioselective production of (*R*)-*o*-chloromandelic acid. *Appl. Environ. Microbiol.* **2015**, *81*, 8469–8477. [CrossRef]
12. Xue, Y.-P.; Wang, Y.-P.; Xu, Z.; Liu, Z.-Q.; Shu, X.-R.; Jia, D.-X.; Zheng, Y.-G.; Shen, Y.-C. Chemoenzymatic synthesis of gabapentin by combining nitrilase-mediated hydrolysis with hydrogenation over Raney-nickel. *Catal. Commun.* **2015**, *66*, 121–125. [CrossRef]
13. Stolz, A.; Eppinger, E.; Sosedov, O.; Kiziak, C. Comparative analysis of the conversion of mandelonitrile and 2-phenylpropionitrile by a large set of variants generated from a nitrilase originating from *Pseudomonas fluorescens* EBC191. *Molecules* **2019**, *24*, 4232. [CrossRef]
14. Bhalla, T.C.; Kumar, V.; Kumar, V.; Thakur, N.; Savitri. Nitrile Metabolizing Enzymes in Biocatalysis and Biotransformation. *Appl. Biochem. Biotechnol.* **2018**, *185*, 925–946. [CrossRef]
15. Rucká, L.; Chmátal, M.; Kulik, N.; Petrásková, L.; Pelantová, H.; Novotný, P.; Příhodová, R.; Pátek, M.; Martínková, L. Genetic and functional diversity of nitrilases in Agaricomycotina. *Int. J. Mol. Sci.* **2019**, *20*, 5990. [CrossRef]
16. Martínková, L.; Bojarová, P.; Sedova, A.; Křen, V. Recent trends in the treatment of cyanide-containing effluents: Comparison of different approaches. *Crit. Rev. Environ. Sci. Technol.* **2023**, *53*, 416–434. [CrossRef]
17. Sharma, M.; Akhter, Y.; Chatterjee, S. A review on remediation of cyanide containing industrial wastes using biological systems with special reference to enzymatic degradation. *World J. Microbiol. Biotechnol.* **2019**, *35*, 70. [CrossRef]
18. Crum, M.A.; Park, J.M.; Mulelu, A.E.; Sewell, B.T.; Benedik, M.J. Probing C-terminal interactions of the *Pseudomonas stutzeri* cyanide-degrading CynD protein. *Appl. Microbiol. Biotechnol.* **2015**, *99*, 3093–3102. [CrossRef]
19. Crum, M.A.; Park, J.M.; Sewell, B.T.; Benedik, M.J. C-terminal hybrid mutant of *Bacillus pumilus* cyanide dihydratase dramatically enhances thermal stability and pH tolerance by reinforcing oligomerization. *J. Appl. Microbiol.* **2015**, *118*, 881–889. [CrossRef]
20. Kumar, V.; Kumar, V.; Bhalla, T.C. Alkaline active cyanide dihydratase of *Flavobacterium indicum* MTCC 6936: Growth optimization, purification, characterization and in silico analysis. *Int. J. Biol. Macromol.* **2018**, *116*, 591–598. [CrossRef]
21. Arevalo, S.J.; Sifuentes, D.Z.; Portocarrero, A.C.; Reategui, M.B.; Pimentel, C.M.; Martins, L.F.; Pierry, P.M.; Piroupo, C.M.; Santa Cruz, A.G.; Aguilar, M.Q.; et al. Genomic characterization of *Bacillus safensis* isolated from mine tailings in Peru and evaluation of its cyanide-degrading enzyme CynD. *Appl. Environ. Microbiol.* **2022**, *88*, e00916-22. [CrossRef]
22. Terada, A.; Komatsu, D.; Ogawa, T.; Flamandita, D.; Sahlan, M.; Nishimura, M.; Yohda, M. Isolation of cyanide-degrading bacteria and molecular characterization of its cyanide-degrading nitrilase. *Biotechnol. Appl. Biochem.* **2022**, *69*, 183–189. [CrossRef] [PubMed]
23. Park, J.M.; Ponder, C.M.; Sewell, B.T.; Benedik, M.J. Residue Y70 of the nitrilase cyanide dihydratase from *Bacillus pumilus* is critical for formation and activity of the spiral oligomer. *J. Microbiol. Biotechnol.* **2016**, *26*, 2179–2183. [CrossRef] [PubMed]
24. Park, J.M.; Mulelu, A.; Sewell, B.T.; Benedik, M.J. Probing an interfacial surface in the cyanide dihydratase from *Bacillus pumilus*, a spiral forming nitrilase. *Front. Microbiol.* **2015**, *6*, 1479. [CrossRef] [PubMed]
25. Sewell, B.T.; Frangakis, A.; Mulelu, A.; Reitz, J. The structure of the cyanide dihydratase (CynD) from *Bacillus pumilus*. *Acta Crystallogr. Sect. A* **2017**, *73*, C1296. [CrossRef]
26. Nolan, L.M.; Harnedy, P.A.; Turner, P.; Hearne, A.B.; O'Reilly, C. The cyanide hydratase enzyme of *Fusarium lateritium* also has nitrilase activity. *FEMS Microbiol. Lett.* **2003**, *221*, 161–165. [CrossRef]
27. Basile, L.J.; Willson, R.C.; Sewell, B.T.; Benedik, M.J. Genome mining of cyanide-degrading nitrilases from filamentous fungi. *Appl. Microbiol. Biotechnol.* **2008**, *80*, 427–435. [CrossRef]

28. Kaplan, O.; Veselá, A.B.; Petříčková, A.; Pasquarelli, F.; Pičmanová, M.; Rinágelová, A.; Bhalla, T.C.; Pátek, M.; Martínková, L. A comparative study of nitrilases identified by genome mining. *Mol. Biotechnol.* **2013**, *54*, 996–1003. [CrossRef]
29. Veselá, A.B.; Rucká, L.; Kaplan, O.; Pelantová, H.; Nešvera, J.; Pátek, M.; Martínková, L. Bringing nitrilase sequences from databases to life: The search for novel substrate specificities with a focus on dinitriles. *Appl. Microbiol. Biotechnol.* **2016**, *100*, 2193–2202. [CrossRef]
30. Sedova, A.; Rucká, L.; Bojarová, P.; Glozlová, M.; Novotný, P.; Křístková, B.; Pátek, M.; Martínková, L. Application potential of cyanide hydratase from *Exidia glandulosa*: Free cyanide removal from simulated industrial effluents. *Catalysts* **2021**, *11*, 1410. [CrossRef]
31. O'Reilly, C.; Turner, P.D. The nitrilase family of CN hydrolysing enzymes—A comparative study. *J. Appl. Microbiol.* **2003**, *95*, 1161–1174. [CrossRef]
32. Rinágelová, A.; Kaplan, O.; Veselá, A.B.; Chmátal, M.; Křenková, A.; Plíhal, O.; Pasquarelli, F.; Cantarella, M.; Martínková, L. Cyanide hydratase from *Aspergillus niger* K10: Overproduction in *Escherichia coli*, purification, characterization and use in continuous cyanide degradation. *Process Biochem.* **2014**, *49*, 445–450. [CrossRef]
33. Sexton, A.C.; Howlett, B.J. Characterisation of a cyanide hydratase gene in the phytopathogenic fungus *Leptosphaeria maculans*. *Mol. Gen. Genet.* **2000**, *263*, 463–470. [CrossRef]
34. Fry, W.E.; Millar, R.L. Cyanide degradation by an enzyme from *Stemphylium loti*. *Arch. Biochem. Biophys.* **1972**, *151*, 468–474. [CrossRef]
35. Barclay, M.; Day, J.C.; Thompson, I.P.; Knowles, C.J.; Bailey, M.J. Substrate-Regulated cyanide hydratase (chy) gene expression in *Fusarium solani*: The potential of a transcription-based assay for monitoring the biotransformation of cyanide complexes. *Environ. Microbiol.* **2002**, *4*, 183–189. [CrossRef]
36. Makumire, S.; Su, S.Y.; Weber, B.W.; Woodward, J.D.; Kimani, S.W.; Hunter, R.; Sewell, B.T. The structures of the C146A variant of the amidase from *Pyrococcus horikoshii* bound to glutaramide and acetamide suggest the basis of amide recognition. *J. Struct. Biol.* **2022**, *214*, 107859. [CrossRef]
37. Weber, B.W.; Kimani, S.W.; Varsani, A.; Cowan, D.A.; Hunter, R.; Venter, G.A.; Gumbart, J.C.; Sewell, B.T. The mechanism of the amidases mutating the glutamate adjacent to the catalytic triad inactivates the enzyme due to substrate mispositioning. *J. Biol. Chem.* **2013**, *288*, 28514–28523. [CrossRef]
38. Křístková, B.; Rädisch, R.; Kulik, N.; Horvat, M.; Rucká, L.; Grulich, M.; Rudroff, F.; Kádek, A.; Pátek, M.; Winkler, M.; et al. Scanning aldoxime dehydratase sequence space and characterization of a new aldoxime dehydratase from *Fusarium vanettenii*. *Enzyme Microb. Technol.* **2023**, *164*, 110187. [CrossRef]
39. Jandhyala, D.M.; Willson, R.C.; Sewell, B.T.; Benedik, M.J. Comparison of cyanide-degrading nitrilases. *Appl. Microbiol. Biotechnol.* **2005**, *68*, 327–335. [CrossRef]
40. Studier, F.W. Protein production by auto-induction in high-density shaking cultures. *Protein Expression Purif.* **2005**, *41*, 207–234. [CrossRef]
41. Gong, J.S.; Zhang, Q.; Gu, B.C.; Dong, T.T.; Li, H.; Li, H.; Lu, Z.M.; Shi, J.S.; Xu, Z.H. Efficient biocatalytic synthesis of nicotinic acid by recombinant nitrilase via high density culture. *Bioresour. Technol.* **2018**, *260*, 427–431. [CrossRef] [PubMed]
42. Xu, C.; Tang, L.; Liang, Y.; Jiao, S.; Yu, H.; Luo, H. Novel chaperones RrGroEL and RrGroES for activity and stability enhancement of nitrilase in *Escherichia coli* and *Rhodococcus ruber*. *Molecules* **2020**, *25*, 1002. [CrossRef] [PubMed]
43. Petříčková, A.; Veselá, A.B.; Kaplan, O.; Kubáč, D.; Uhnáková, B.; Malandra, A.; Felsberg, J.; Rinágelová, A.; Weyrauch, P.; Křen, V.; et al. Purification and characterization of heterologously expressed nitrilases from filamentous fungi. *Appl. Microbiol. Biotechnol.* **2012**, *93*, 1553–1561, Erratum in *Appl. Microbiol. Biotechnol.* **2013**, *97*, 9263–9264. [CrossRef] [PubMed]
44. Lévy-Schil, S.; Soubrier, F.; Crutz-Le Coq, A.M.; Faucher, D.; Crouzet, J.; Pétré, D. Aliphatic nitrilase from a soil-isolated *Comamonas testosteroni* sp.: Gene cloning and overexpression, purification and primary structure. *Gene* **1995**, *161*, 15–20. [CrossRef]
45. Crum, M.A.; Sewell, B.T.; Benedik, M.J. *Bacillus pumilus* cyanide dihydratase mutants with higher catalytic activity. *Front. Microbiol.* **2016**, *7*, 1264. [CrossRef]
46. Shen, Q.; Yu, Z.; Lv, P.J.; Li, Q.; Zou, S.P.; Xiong, N.; Liu, Z.Q.; Xue, Y.P.; Zheng, Y.G. Engineering a *Pichia pastoris* nitrilase whole cell catalyst through the increased nitrilase gene copy number and co-expressing of ER oxidoreductin 1. *Appl. Microbiol. Biotechnol.* **2020**, *104*, 2489–2500. [CrossRef]
47. Rustler, S.; Motejadded, H.; Altenbuchner, J.; Stolz, A. Simultaneous expression of an arylacetonitrilase from *Pseudomonas fluorescens* and a (*S*)-oxynitrilase from *Manihot esculenta* in *Pichia pastoris* for the synthesis of (*S*)-mandelic acid. *Appl. Microbiol. Biotechnol.* **2008**, *80*, 87–97. [CrossRef]
48. Zhang, X.; Wang, C.; Ge, Y.; Meng, Q.; Zhang, Y. Constitutive secretory expression and characterization of nitrilase from *Alcaligenes faecalis* in *Pichia pastoris* for production of *R*-mandelic acid. *Biotechnol. Appl. Biochem.* **2021**, *69*, 587–595. [CrossRef]
49. Kuyucak, N.; Akcil, A. Cyanide and removal options from effluents in gold mining and metallurgical processes. *Miner. Eng.* **2013**, *50–51*, 13–29. [CrossRef]
50. Cluness, M.J.; Turner, P.D.; Clements, E.; Brown, D.T.; Oreilly, C. Purification and properties of cyanide hydratase from *Fusarium lateritium* and analysis of the corresponding *chy1* gene. *J. Gen. Microbiol.* **1993**, *139*, 1807–1815. [CrossRef]
51. Olsen, B.A. Hydrophilic interaction chromatography using amino and silica columns for the determination of polar pharmaceuticals and impurities. *J. Chromatogr. A* **2001**, *913*, 113–122. [CrossRef]

52. Jandhyala, D.; Berman, M.; Meyers, P.R.; Sewell, B.T.; Willson, R.C.; Benedik, M.J. CynD, the cyanide dihydratase from *Bacillus pumilus*: Gene cloning and structural studies. *Appl. Environ. Microbiol.* **2003**, *69*, 4794–4805. [CrossRef]
53. Sewell, B.T.; Berman, M.N.; Meyers, P.R.; Jandhyala, D.; Benedik, M.J. The cyanide degrading nitrilase from *Pseudomonas stutzeri* AK61 is a two-fold symmetric, 14-subunit spiral. *Structure* **2003**, *11*, 1413–1422. [CrossRef]
54. Mulelu, A.E.; Kirykowicz, A.M.; Woodward, J.D. Cryo-EM and directed evolution reveal how *Arabidopsis* nitrilase specificity is influenced by its quaternary structure. *Commun. Biol.* **2019**, *2*, 260. [CrossRef]
55. Sewell, B.T.; Thuku, R.N.; Zhang, X.; Benedik, M.J. Oligomeric structure of nitrilases—Effect of mutating interfacial residues on activity. In *Natural Products and Molecular Therapy*; Kotwal, G.J., Lahiri, D.K., Eds.; Annals of the New York Academy of Sciences: Wiley, Hoboken, NJ, USA, 2005; Volume 1056, pp. 153–159.
56. Zhang, L.; Yin, B.; Wang, C.; Jiang, S.; Wang, H.; Yuan, Y.A.; Wei, D. Structural insights into enzymatic activity and substrate specificity determination by a single amino acid in nitrilase from *Syechocystis* sp. PCC6803. *J. Struct. Biol.* **2014**, *188*, 93–101. [CrossRef]
57. Xu, Z.; Cai, T.; Xiong, N.; Zou, S.P.; Xue, Y.P.; Zheng, Y.G. Engineering the residues on "A" surface and C-terminal region to improve thermostability of nitrilase. *Enzyme Microb. Technol.* **2018**, *113*, 52–58. [CrossRef]
58. Jiang, S.Q.; Zhang, L.J.; Yao, Z.Q.; Gao, B.; Wang, H.L.; Mao, X.Z.; Wei, D.Z. Switching a nitrilase from *Syechocystis* sp. PCC6803 to a nitrile hydratase by rationally regulating reaction pathways. *Catal. Sci. Technol.* **2017**, *7*, 1122–1128. [CrossRef]
59. Wang, L.; Watermeyer, J.M.; Mulelu, A.E.; Sewell, B.T.; Benedik, M.J. Engineering pH-tolerant mutants of a cyanide dihydratase. *Appl. Microbiol. Biotechnol.* **2012**, *94*, 131–140. [CrossRef]
60. Zhang, Q.; Lu, X.F.; Zhang, Y.; Tang, X.L.; Zheng, R.C.; Zheng, Y.G. Development of a robust nitrilase by fragment swapping and semi-rational design for efficient biosynthesis of pregabalin precursor. *Biotechnol. Bioeng.* **2020**, *117*, 318–329. [CrossRef]
61. Martínková, L.; Chmátal, M. The integration of cyanide hydratase and tyrosinase catalysts enables effective degradation of cyanide and phenol in coking wastewaters. *Water Res.* **2016**, *102*, 90–95. [CrossRef]
62. Carmona-Orozco, M.L.; Panay, A.J. Immobilization of *E. coli* expressing *Bacillus pumilus* CynD in three organic polymer matrices. *Appl. Microbiol. Biotechnol.* **2019**, *103*, 5401–5410. [CrossRef] [PubMed]
63. Kumar, V.; Kumar, V.; Singh, A.K.; Verma, N.; Bhalla, T.C. A potentiometric biosensor for cyanide detection using immobilized whole cell cyanide dihydratase of *Flavobacterium indicum* MTCC 6936. *J. Anal. Chem.* **2018**, *73*, 1014–1019. [CrossRef]
64. Wang, X.C.; Davis, I.; Liu, A.M.; Miller, A.; Shamsi, S.A. Improved separation and detection of picolinic acid and quinolinic acid by capillary electrophoresis-mass spectrometry: Application to analysis of human cerebrospinal fluid. *J. Chromatogr. A* **2013**, *1316*, 147–153. [CrossRef] [PubMed]
65. Xu, Z.; Huang, J.W.; Xia, C.L.; Zou, S.P.; Xue, Y.P.; Zheng, Y.G. Enhanced catalytic stability and reusability of nitrilase encapsulated in ethyleneamine-mediated biosilica for regioselective hydrolysis of 1-cyanocycloalkaneacetonitrile. *Int. J. Biol. Macromol.* **2019**, *130*, 117–124. [CrossRef] [PubMed]
66. Forsyth, C.; Yip, T.W.S.; Patwardhan, S.V. CO_2 sequestration by enzyme immobilized onto bioinspired silica. *Chem. Commun.* **2013**, *49*, 3191–3193. [CrossRef]
67. Khatik, A.G.; Jain, A.K.; Muley, A.B. Preparation, characterization and stability of cross linked nitrilase aggregates (nitrilase-CLEAs) for hydroxylation of 2-chloroisonicotinonitrile to 2-chloroisonicotinic acid. *Bioprocess Biosyst. Eng.* **2022**, *45*, 1559–1579. [CrossRef]
68. Sheldon, R.A. Cross-linked enzyme aggregates as industrial biocatalysts. *Org. Process Res. Dev.* **2011**, *15*, 213–223. [CrossRef]
69. Sheldon, R.A.; Schoevaart, R.; Van Langen, L.M. Cross-linked enzyme aggregates (CLEAs): A novel and versatile method for enzyme immobilization (a review). *Biocatal. Biotransform.* **2005**, *23*, 141–147. [CrossRef]
70. Jones, D.T.; Taylor, W.R.; Thornton, J.M. The rapid generation of mutation data matrices from protein sequences. *Comput. Appl. Biosci.* **1992**, *8*, 275–282. [CrossRef]
71. Gascuel, O. BIONJ: An improved version of the NJ algorithm based on a simple model of sequence data. *Mol. Biol. Evol.* **1997**, *14*, 685–695. [CrossRef]
72. Tamura, K.; Peterson, D.; Peterson, N.; Stecher, G.; Nei, M.; Kumar, S. MEGA5: Molecular Evolutionary Genetics Analysis Using Maximum Likelihood, Evolutionary Distance, and Maximum Parsimony Methods. *Mol. Biol. Evol.* **2011**, *28*, 2731–2739. [CrossRef]
73. Kumar, S.; Stecher, G.; Li, M.; Knyaz, C.; Tamura, K. MEGA X: Molecular evolutionary genetics analysis across computing platforms. *Mol. Biol. Evol.* **2018**, *35*, 1547–1549. [CrossRef]
74. Letunic, I.; Bork, P. Interactive Tree Of Life (iTOL) v5: An online tool for phylogenetic tree display and annotation. *Nucleic Acids Res.* **2021**, *49*, W293–W296. [CrossRef]